Second Order Washout filter based Power Sharing Strategy for Uninterruptible Power Supply

Lu, Jinghang; Savaghebi, Mehdi; Guerrero, Josep M.

Published in:
Proceedings of 43rd Annual Conference of the IEEE Industrial Electronics Society, IECON 2017

DOI (link to publication from Publisher):
10.1109/IECON.2017.8217376

Publication date:
2017

Document Version
Early version, also known as pre-print

Second Order Washout filter based Power Sharing Strategy for Uninterruptible Power Supply

Jinghang Lu, Mehdi Savaghebi, Josep M.Guerrero
Department of Energy Technology
Aalborg University, Denmark
{jgl,mes,joz}@et.aau.dk

***Abstract*—In this paper, first, the existing frequency and voltage amplitude restoration control strategies are reviewed. Moreover, the proposed second order washout filter control strategy is proposed to enhance the dynamic response under load disturbance. The physical parameter of the proposed method is derived, and system stability for the system parameter is discussed. Finally, extensive simulation results are provided to verify the effectiveness of the proposed method for UPS system.**

***Keywords*—UPS; second order washout filter; secondary control**

I. Introduction

The Uninterruptible Power Supply (UPS) systems have recently experienced a large demand as the investment on the critical loads, such as: data center, financial institution, personal computers and healthcare facilities, is dramatically increased. These critical loads, which require reliable, secure and efficient power supply, are usually connected to the grid by the UPSs, since the UPSs are able to protect the critical loads from the power outages, surges and other issues from the grid [1].

According to the European Standard EN 62040-3[2], the UPS systems are categorized into on-line, off-line and line-interactive UPSs. The on-line UPS system is receiving more intention from the engineers and researchers because of its excellent capability of being immune to the grid frequency variation, voltage irregularity and other power issues.

Normally, an on-line UPS system consists of a rectifier, an inverter, a battery and a static bypass switch [3]. The rectifier is in charge of the power delivery from the utility to the DC link, and the inverter is responsible for the power transfer from the DC link to the critical load. Note that the battery is usually fully charged and operates in “standby” mode in the normal mode of operation. In case of overloading or UPS failure, the bypass switch needs to be closed and the load power is directly supplied the by the utility. To achieve more reliable power supply to the sensitive loads, multiple inverters are operating together to supply the power to the critical load, as shown in Fig.1.

For the normal operation of the parallel UPS system, several control strategies have been adopted, such as the master-slave control [4], the average load sharing control [5], and the circular chain control to allow the inverter modules to share the active and reactive power of the load. However, in these methods, the intercommunication system is mandatory in the control strategy. In order to avoid the communication system, the wireless droop control [6] has been proposed to avoid the critical communication to achieve the active and reactive power sharing. However, the frequency and voltage amplitude deviation is inevitable in the steady state, and dynamic stability is poor for the power sharing. In order to deal with the above issue, the improved droop control strategy [7] have been proposed to realize the power decoupling and ensure system stability. However, the system stability model is incomplete without considering the voltage and current loop controller in the modeling.

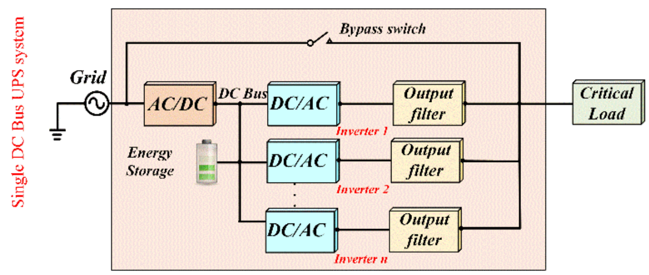

Fig.1. Structure of parallel UPS system

Recently, the central or distributed secondary controller have been employed to compensate the frequency and voltage amplitude deviation [8-10]. In addition, the consensus-based secondary control strategy [11] is presented to achieve the accurate power sharing. With this control strategy, only the inverter’s own information and its neighbor’s information are needed. The multi-agent(MAS) [12], graph theory, and predictive control strategies [13] are adopted to improve the stability and accuracy of the power sharing under the complex environment. However, these methods usually adopts the low-bandwidth communication (LBC) lines, the output signals of these controller that sent to the primary control layer are always along with the time delay[14]. As a result, controller can not have fast response that degrades the system performance.

In order to overcome the time delay effect of the LBC line, several works have been presented, and among these works, a model predictive and smith predictor-based control strategy [15] is implemented to reduce the influence of delay caused by the LBC lines. In [14], the gain schedule method is implemented to minimize the delay’s effect. However, the complicated strategy decreased the reliability and stability of the system. Recently, the first order washout filter (FOWF)-based control strategy[16,17] is proposed in the primary control layer to recover the frequency and the amplitude deviation caused by the droop control strategy. This control strategy is demonstrated to be equivalent to the

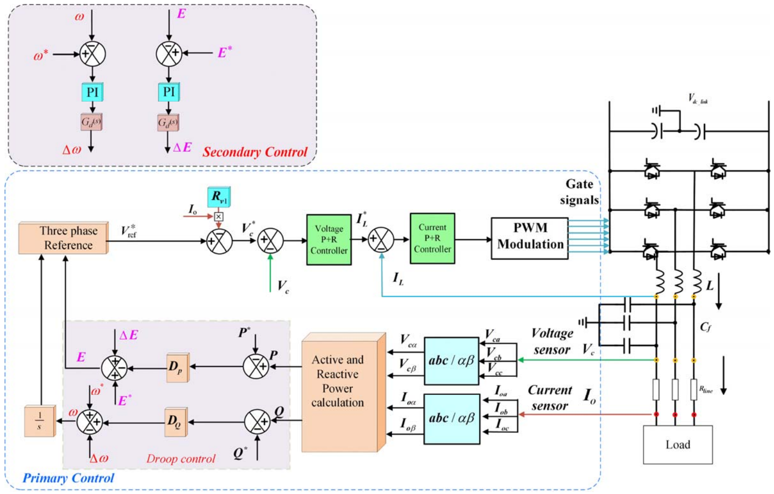

Fig.2. Complete block diagram of the UPS system with the seconary control.

Proportional-Integral (PI) controller-based secondary control strategy. However, in [16, 17], the system dynamic response under the load disturbance is still quite slow, which may not satisfy the requirement of sensitive loads in the UPS system. As the small frequency and the amplitude deviation along with the fast restoration are required for the UPS system.

In this paper, first, the equivalent model between the FOWF and the secondary control strategy is reviewed. In order to increase system dynamic response, a Second Order Washout Filter (SOWF) based control strategy will be proposed, the equivalence between the secondary control with lead filter and the SOWF-based control strategy is verified by the analysis. Furthermore, the analysis of critical parameter for the SOWF control strategy on the system stability is discussed. The feasibility and effectiveness of the proposed method are validated by the simulation.

II. Review of Existing Methods

In the parallel UPS system, the secondary control strategy is adopted to restore the frequency and the voltage amplitude deviation caused by the droop control strategy. When the *LC* type output filter is applied in the UPS system, the $Q-\omega$, *P-E* control strategy is implemented for the active and reactive power sharing and expressed as:

$$\omega = \omega^* + D_Q(Q_{LPF} - Q^*) \tag{1}$$

$$E = E^* - D_p(P_{LPF} - P^*) \tag{2}$$

where ω^* and ω are the UPS nominal and reference angular frequency, E^* and E are the UPS nominal and reference voltage amplitude. D_p and D_Q are the droop coefficients for regulating the UPS active power and reactive power, respectively. Q^* and P^* are the reactive and active power reference, respectively. Normally, these references are set to be zero.

A. Secondary control strategy

The droop control strategy manages to regulate the frequency and the voltage amplitude for the voltage reference to achieve the active and reactive power sharing. However, the amplitude and frequency may deviate from its nominal value when applying the droop control strategy, and these deviations may thus be harmful to the sensitive critical load. Moreover, the influence of the disturbances, such as the load connection/disconnection leads to the poor dynamic stability of active power sharing. Hence, in order to deal with the above mentioned issue in the traditional droop control strategy, a secondary control strategy has been adopted to recover the frequency and voltage amplitude of the UPS system and improve the system stability. The details of the secondary control strategy is illustrated in Fig.2, where a low bandwidth communication among the UPS modules are implemented to share frequency and voltage amplitude. In the secondary control layer, the PI controller are used to respectively recover the frequency and voltage amplitude deviation and expressed as:

$$\omega_{sec} = G_{\omega,sec}(\omega^* - \omega) \tag{3}$$

$$E_{sec} = G_{E,sec}(E^* - E) \tag{4}$$

where $G_{\omega,sec} = k_{p\omega} + \frac{k_{i\omega}}{s}$, $G_{E,sec} = k_{pE} + \frac{k_{iE}}{s}$, $k_{p\omega}$ and $k_{i\omega}$ are the control parameters of the PI compensator in the frequency restoration. k_{pE} and k_{iE} are the control parameters of the PI compensator in the voltage amplitude restoration. The output of the PI controller ω_{sec} and E_{sec} are sent to the droop control strategy in the primary control layer to restore the nominal voltage frequency and amplitude value. Note that the secondary control strategy requires all the UPS modules to communicate with each other. However, due to the communication lost, and delay's effect in the low bandwidth communication system, accurate reactive power sharing and fast dynamic response of the system may be not achieved . Recently, the washout filter based control strategy is proposed for restoration of the frequency and voltage amplitude. And it shows the effective way to compensate the frequency and voltage amplitude deviation. In the next section, the washout filter based control strategy will be reviewed.

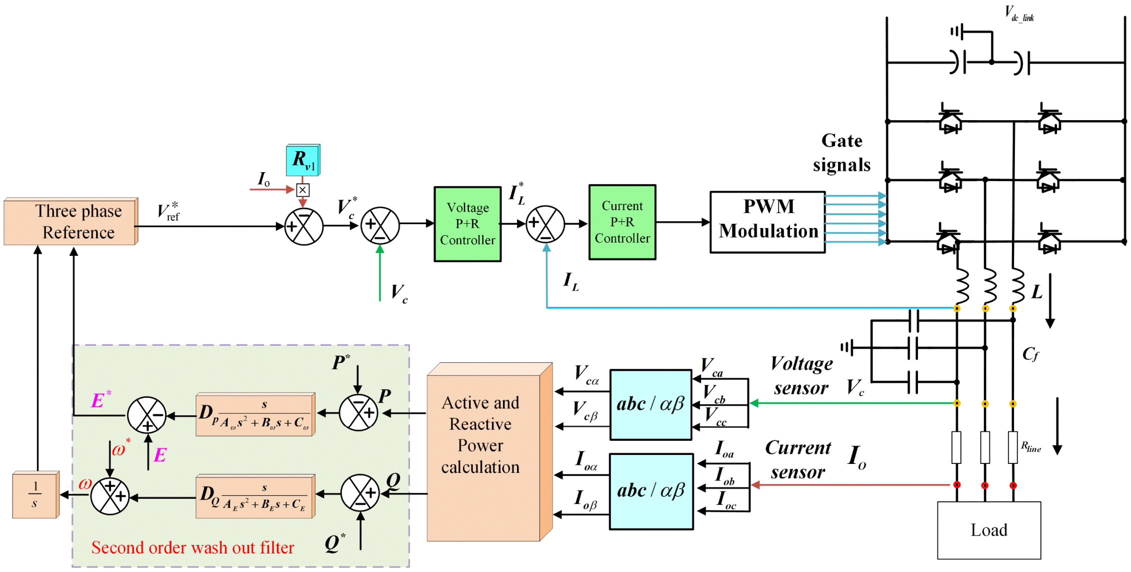

Fig.3. Complete diagram of the UPS module with the proposed control method

B. Washout filter based control strategy.

In order to eliminate the delay's effect on the low bandwidth communication system when restoring the frequency and voltage amplitude deviation, a washout filter based power sharing strategy has been proposed to share the active and reactive power sharing. The principle is illustrated as follows: by time derivative of (1) and (2), the following equations are obtained:

$$\frac{d}{dt}\Delta\omega - D_Q\frac{d}{dt}\Delta Q = 0 \quad (5)$$

$$\frac{d}{dt}\Delta E + D_Q\frac{d}{dt}\Delta P = 0 \quad (6)$$

where $\Delta\omega = \omega - \omega^*$, $\Delta Q = Q_{LPF} - Q^*$, $\Delta E = E - E^*$, $\Delta P = P_{LPF} - P^*$.

By adding a factor of $\Delta\omega$ in (5) and ΔE in (6), the following equations are derived and expressed as:

$$\frac{d}{dt}\Delta\omega - D_Q\frac{d}{dt}\Delta Q + k_Q\Delta\omega = 0 \quad (7)$$

$$\frac{d}{dt}\Delta E + D_Q\frac{d}{dt}\Delta P + k_P\Delta E = 0 \quad (8)$$

In the steady state, the derivative terms of (7) and (8) are zero, which means $\frac{d}{dt}\Delta\omega = 0, \frac{d}{dt}\Delta Q = 0, \frac{d}{dt}\Delta E = 0, \frac{d}{dt}\Delta P = 0$. Therefore, (7) and (8) forces $\Delta\omega$ and ΔE to be zero in the steady state, which indicates that the voltage amplitude and the frequency restore to its nominal value. When (7) and (8) are expressed in s-domain, they are expressed as:

$$\omega = \omega^* + D_Q\frac{s}{s+k_Q}(Q_{LPF} - Q^*) \quad (9)$$

$$E = E^* - D_p\frac{s}{s+k_P}(P_{LPF} - P^*) \quad (10)$$

where k_P and k_Q are the control parameters of the washout filter. By using the washout filter control strategy, secondary controller can be replaced with the washout filter to recover the frequency and voltage amplitude.

However, with the first order washout filter based control strategy, the system response under disturbance is still quite slow, which may not satisfy the requirement for sensitive loads in the UPS system that needs small frequency and amplitude deviation and fast restoration. Therefore, a SOWF-based control strategy is presented in this section to further improve the system dynamic response

III. SECOND ORDER WASHOUT FILTER CONTROL STRATEGY

The complete control diagram of each UPS module is shown in Fig.3, where it is seen that the outer loop voltage controller is adopted for regulating the output filter's capacitor voltage, and the current control strategy is nested inside the voltage regulation loop to directly control the inductor's current and limit the current during the transient as a protection method. Finally, the proposed SOWF-based control strategy is implemented for voltage and frequency restoration to replace the secondary control strategy. In the following part, the SOWF strategy will be illustrated in detail.

The proposed SOWF-based control strategy is shown as:

$$\omega = \omega^* + D_q\frac{s}{A_\omega s^2 + B_\omega s + C_\omega}Q \quad (11)$$

$$E = E^* - D_p\frac{s}{A_E s^2 + B_E s + C_E}P \quad (12)$$

where D_p and D_q are the droop coefficient, A_ω B_ω and C_ω are the SOWF frequency parameter, A_E, B_E and C_E are the SOWF voltage amplitude parameter. By implementing the proposed control strategy, the secondary control strategy is omitted and the communication delays caused by low bandwidth communication (LBC) line is solved. The relationship between the SOWF control strategy and secondary PI control strategy will be analyzed in the following of this section:

Normally, the secondary control strategy that consists of a PI controller is derived as:

$$\omega_{sec} = G_{\omega,sec}G_d(\omega^* - \omega) \quad (13)$$

$$E_{sec} = G_{E,sec} G_d (E^* - E) \tag{14}$$

where $G_{\omega,sec} = k_{p\omega} + \frac{k_{i\omega}}{s}$, $G_{E,sec} = k_{pE} + \frac{k_{iE}}{s}$, $G_d = e^{-T_d s} = \frac{1}{1+T_d s}$ is defined as the LBC line delay, Moreover, the traditional droop control strategy with secondary control are expressed as:

$$\omega = \omega^* + D_q G_{LPF}(s) q + \omega_{sec} \tag{15}$$

$$E = E^* - D_p G_{LPF}(s) p + E_{sec} \tag{16}$$

where G_{LPF} is the low pass filter, $P = G_{LPF}(s)p$, $Q = G_{LPF}(s)q$, p and q are instantaneous power. By combining (13) and (15), (14) and (16) respectively, the following expression is derived:

$$\omega = \omega^* + D_q G_{LPF}(s) \frac{1}{1+G_{\omega,sec} G_d} q \tag{17}$$

$$E = E^* - D_p G_{LPF}(s) \frac{1}{1+G_{E,sec} G_d} p \tag{18}$$

In the secondary control, in order to compensate for the delay's effect, ideally, the lead filter $G_d^{-1} = 1 + T_d s$ should be adopted, which is expressed as:

$$\omega = \omega^* + D_q G_{LPF}(s) \frac{1}{1+G_{\omega,sec} G_d (1+T_d s)} q \tag{19}$$

$$E = E^* - D_p G_{LPF}(s) \frac{1}{1+G_{E,sec} G_d (1+T_d s)} p \tag{20}$$

However, in reality, the actual delay is unknown, but from practical view of point, the delay is ranged from hundreds of mill second to second, therefore, the T_d is usually choosed as 0.1~1. Finally, as the SOWF is implemented in primary control, the unknown delay G_d is neglected and expressed as $G_d = 1$. Therefore, the second-order washout filter is derived as:

$$\omega = \omega^* + D_q G_{LPF}(s) \frac{1}{1 + \left(k_{p\omega} + \frac{k_{i\omega}}{s}\right)(1 + T_d s)} q$$
$$= \omega^* + D_q G_{LPF}(s) \frac{s}{A_\omega s^2 + B_\omega s + C_\omega} q \tag{21}$$

where $A_\omega = k_{p\omega} T_d$, $B_\omega = 1 + k_{p\omega} + k_{p\omega} T_d$, $C_\omega = k_{i\omega}$

$$E = E^* - D_p G_{LPF}(s) \frac{1}{1 + \left(k_{pE} + \frac{k_{iE}}{s}\right)(1 + T_d s)} p$$
$$= E^* - D_p G_{LPF}(s) \frac{s}{A_E s^2 + B_E s + C_E} p \tag{22}$$

where $A_E = k_{pE} T_d$, $B_E = 1 + k_{pE} + k_{pE} T_d$, $C_E = k_{iE}$.

By comparing the proposed SOWF control strategy with the traditional secondary control strategy, it is observed that the SOWF includes the traditional PI control strategy of the secondary control layer and adds a lead filter to accelerate the dynamic response. However, as the SOWF is implemented in the primary control layer, the delay's effect does not exist anymore. Moreover, by comparing the proposed SOWF method with the first order washout filter in [16], it is seen that [16] is a special case when $T_d = 0$. In order to avoid the signal p and q to go through an ill-conditioned filter. The bandwidth of the SOWF should be smaller than that of low pass filter $G_{LPF}(s)$. The system stability and system parameter design will be discussed in the next section.

IV. STABILITY OF THE PROPOSED METHOD

In this section, the system stability is analyzed with the proposed SOWF-based control strategy. In the following section, the washout parameter will be explored to see the frequency restoration process and voltage amplitude restoration process.

For the SOWF frequency droop control strategy, the dynamic model between ω and reactive power Q is expressed as:

$$\frac{Q}{\omega} = D_q \frac{1}{1+\left(k_{p\omega}+\frac{k_{i\omega}}{s}\right)(1+T_d s)} \tag{23}$$

The pole-zero map under the different control parameter is presented in Fig.4. As is seen from Fig.4 (a), when the $k_{p\omega}$ increases from 0.1 to 4, one dominant pole moves to the right but converges into a stable point that still have distance from the imaginary axis. Another pole moves to the right as well. As this pole is quite far from the imaginary axis, Its influence on the stability of the system is neglected. Meanwhile, $k_{i\omega}$ increases from 0.1 to 4, One pole moves into the left-infinity, the other dominant pole move towards to the left as well but converges into a stable point (see Fig.4 (b)). Finally, the parameter T_d varies from 0.1 to 2, as is seen from Fig.4 (c), both of these two poles move to a stable point. From above analysis, it is found that in order to have a good performance for SOWF controller, $k_{p\omega}$ should be chosen between 0.2-0.5, $k_{i\omega}$ is chosen greater than 4. And T_d is chosen to be less than 0.5.

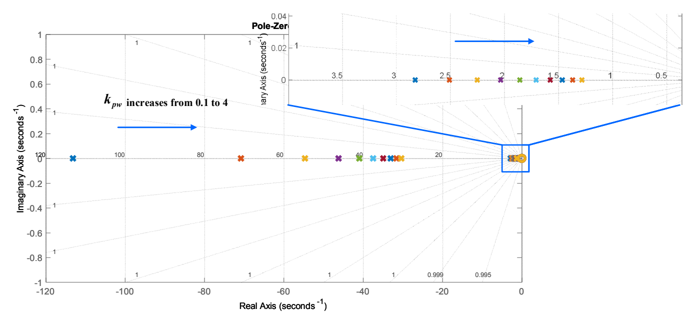

(a) p-z map with variable $k_{p\omega}$

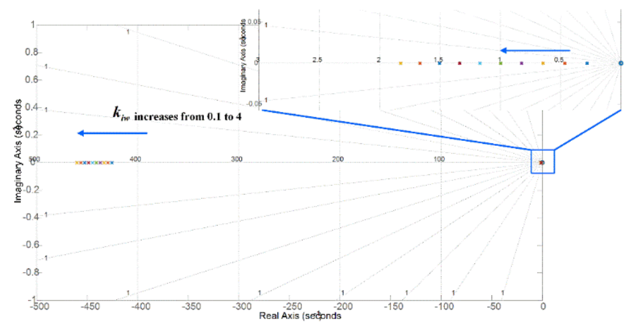

(b) p-z map with variable $k_{i\omega}$

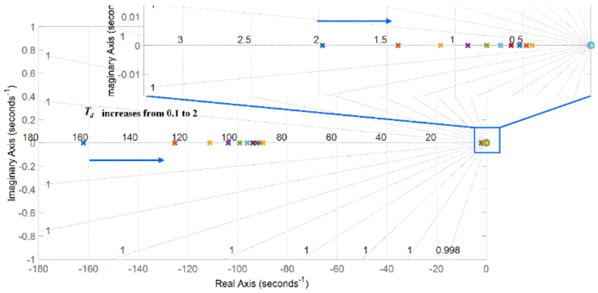

(c) p-z map with variable T_d

Fig.4. Pole-zero map of the frequency restoration.

V. SIMULATION

In this section, the dynamic response for the SOWF based control strategy will be compared with the secondary controller with LBC delay, and FOWF based control strategy that was proposed in [16].

The system parameters are shown in Table I. It is noted that parameter of $k_{p\text{E}}$, $k_{i\text{E}}$, $k_{p\omega}$ and $k_{i\omega}$ are chosen the same parameter for these three methods.

TABLE I. SYSTEM PARAMETERS

System Parameter	
Filter Inductor L_f	$1.8mH$
ESR of Inductor	0.02ohm
Filter Capacitor C_f	$27uF$
Sampling frequency	10kHz
Droop Coefficient	
Frequency droop D_q	0.0001
Voltage droop D_p	0.00005
Voltage Control Parameter	
Proportional gainK_{pv}	0.2
Resonant gain K_{iv}	100
Current controller Parameter	
Proportional K_{p_i}	5.6
Resonant gain K_{i_i}	500

The performance of the secondary control strategy that is applied to the UPS system is shown in Fig.5. In this control strategy, two sample delay is applied for the secondary control. Initially, the two UPS modules are providing the active power (6.5kW) and reactive power (10kVar) to the load 1. As is seen from Fig.5 (c) and (d), at 0.3s when the Load 2 is connected with Load 1, it takes over 1.5s for the frequency recovery during the transient time. Moreover, the frequency deviate from 314.16 rad/s to 314.18 rad/s during the transient time. Meanwhile, the voltage amplitude recovery time takes around 0.7s, and voltage amplitude drops 0.5V from the nominal value during the transient process.

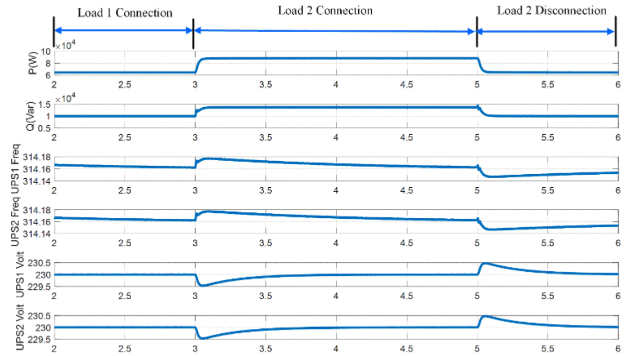

Fig.5. Dynamic response for UPS modules for secondary control with LBC delay(a) Active power, (b) Reactive power (c)Frequency for UPS 1 (d) Frequency for UPS 2 (e) Voltage amplitude for UPS 1 (f) Voltage amplitude for UPS 2

The dynamic response of the FOWF-based control strategy is shown in Fig.6. At first only load 1 is connected and load 2 is connected with load 1 at 3s, From Fig.6 (c) and (d) it is found that the transient error for frequency reduced 1% compared with Fig.5 (c) and (d). Meanwhile, the time to eliminate the frequency deviation takes 0.5s. From Fig.6 (e) and (f) it is shown that the voltage amplitude deviation with FOWF is same with the secondary control Fig.5(e) and (f).

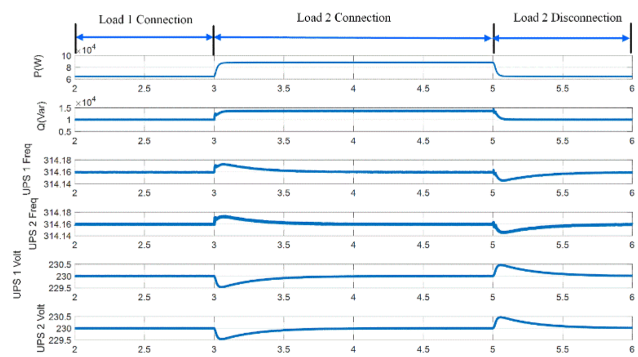

Fig.6. Dynamic response for UPS modules with First order washout filter based control strategy (a) Active power, (b) Reactive power (c)Frequency for UPS 1 (d) Frequency for UPS 2 (e) Voltage amplitude for UPS 1 (f) Voltage amplitude for UPS 2

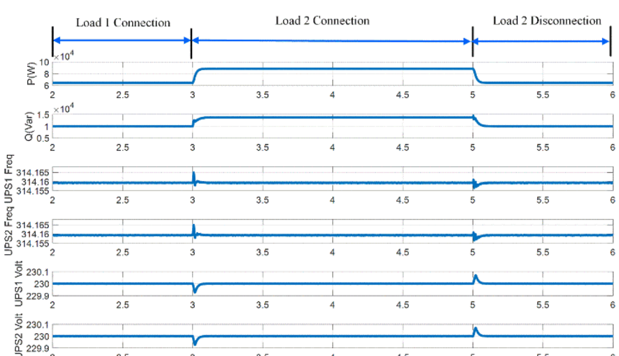

Fig.7. Dynamic response for UPS modules with Second order washout filter based control strategy (a) Active power, (b) Reactive power (c)Frequency

for UPS 1 (d) Frequency for UPS 2 (e) Voltage amplitude for UPS 1 (f) Voltage amplitude for UPS 2

When the SOWF is applied for frequency and voltage amplitude restoration, as is shown in Fig.7, at 3s, the restoration time for frequency is greatly reduced from around 0.7s to less than 0.1s. Moreover, the frequency fluctuation is further dropped to 0.005Hz as well (Fig.7 (c) and (d)). In addition, the voltage amplitude recovery time is less than 0.1s and amplitude deviation is less than 0.1V (Fig.7 (e) and (f)) that is in contrast with the previous two methods. Finally, it is noted that due to the immunity of LBC delay, FOWF and SOWF can both achieve frequency and voltage amplitude restoration without communication lines. However, the dynamic response is significantly improved for SOWF.

VI. Conclusion

In this paper, the second order washout filter based strategy is proposed to increase the dynamic response under load disturbance. Compared with the existing method, the SOWF control strategy by adding a lead filter dramatically enhance the dynamic response under load. Simulation results validate the effectiveness of the proposed methods.

References

[1] M. S. Racine, J. D. Parham, and M. H. Rashid, "An overview of uninterruptible power supplies," in *Proceedings of the 37th Annual North American Power Symposium, 2005.*, 2005, pp. 159-164.

[2] "EN 62040-3 Uninterruptible power systems (UPS) – Part 3: Method of specifying the performance and test requirements."

[3] C. Zhang, J. M. Guerrero, J. C. Vasquez, and E. A. A. Coelho, "Control Architecture for Parallel-Connected Inverters in Uninterruptible Power Systems," *IEEE Transactions on Power Electronics,* vol. 31, no. 7, pp. 5176-5188, 2016.

[4] P. Yunqing, J. Guibin, Y. Xu, and W. Zhaoan, "Auto-master-slave control technique of parallel inverters in distributed AC power systems and UPS," in *Power Electronics Specialists Conference, 2004. PESC 04. 2004 IEEE 35th Annual*, 2004, vol. 3, pp. 2050-2053 Vol.3.

[5] S. Xiao, L. Yim-Shu, and X. Dehong, "Modeling, analysis, and implementation of parallel multi-inverter systems with instantaneous average-current-sharing scheme," *IEEE Transactions on Power Electronics,* vol. 18, no. 3, pp. 844-856, 2003.

[6] C. T. Lee, C. C. Chu, and P. T. Cheng, "A New Droop Control Method for the Autonomous Operation of Distributed Energy Resource Interface Converters," *Power Electronics, IEEE Transactions on,* vol. 28, no. 4, pp. 1980-1993, 2013.

[7] T. Wu, Z. Liu, J. Liu, S. Wang, and Z. You, "A Unified Virtual Power Decoupling Method for Droop-Controlled Parallel Inverters in Microgrids," *IEEE Transactions on Power Electronics,* vol. 31, no. 8, pp. 5587-5603, 2016.

[8] Q. Shafiee, J. M. Guerrero, and J. C. Vasquez, "Distributed Secondary Control for Islanded Microgrids—A Novel Approach," *Power Electronics, IEEE Transactions on,* vol. 29, no. 2, pp. 1018-1031, 2014.

[9] J. C. Vasquez, J. M. Guerrero, M. Savaghebi, J. Eloy-Garcia, and R. Teodorescu, "Modeling, Analysis, and Design of Stationary-Reference-Frame Droop-Controlled Parallel Three-Phase Voltage Source Inverters," *Industrial Electronics, IEEE Transactions on,* vol. 60, no. 4, pp. 1271-1280, 2013.

[10] M. Savaghebi, A. Jalilian, J. C. Vasquez, and J. M. Guerrero, "Secondary Control for Voltage Quality Enhancement in Microgrids," *Smart Grid, IEEE Transactions on,* vol. 3, no. 4, pp. 1893-1902, 2012.

[11] D. He, D. Shi, and R. Sharma, "Consensus-based distributed cooperative control for microgrid voltage regulation and reactive power sharing," in *IEEE PES Innovative Smart Grid Technologies, Europe*, 2014, pp. 1-6.

[12] Q. Li, F. Chen, M. Chen, J. M. Guerrero, and D. Abbott, "Agent-Based Decentralized Control Method for Islanded Microgrids," *IEEE Transactions on Smart Grid,* vol. 7, no. 2, pp. 637-649, 2016.

[13] Y. Zhang, R. Wang, T. Zhang, Y. Liu, and B. Guo, "Model predictive control-based operation management for a residential microgrid with considering forecast uncertainties and demand response strategies," *IET Generation, Transmission & Distribution,* vol. 10, no. 10, pp. 2367-2378, 2016.

[14] S. Liu, X. Wang, and P. X. Liu, "Impact of Communication Delays on Secondary Frequency Control in an Islanded Microgrid," *IEEE Transactions on Industrial Electronics,* vol. 62, no. 4, pp. 2021-2031, 2015.

[15] C. Ahumada, R. Cárdenas, D. Sáez, and J. M. Guerrero, "Secondary Control Strategies for Frequency Restoration in Islanded Microgrids With Consideration of Communication Delays," *IEEE Transactions on Smart Grid,* vol. 7, no. 3, pp. 1430-1441, 2016.

[16] H. A. N. Y, H. Li, L. Xu, X. Zhao, and J. Guerrero, "Analysis of Washout Filter-Based Power Sharing Strategy——An Equivalent Secondary Controller For Islanded Microgrid without LBC Lines," *IEEE Transactions on Smart Grid,* vol. PP, no. 99, pp. 1-1, 2017.

[17] M. Yazdanian and A. Mehrizi-Sani, "Washout Filter-Based Power Sharing," *IEEE Transactions on Smart Grid,* vol. 7, no. 2, pp. 967-968, 2016.